Ab Initio Derivation of Stress and Strain in Fluid Foams

Y. Jiang
Theoretical Division, Los Alamos National Laboratory, Los Alamos, NM 87545, USA
jiang@lanl.gov
M. Asipauskas, J. A. Glazier
Department of Physics, University of Notre Dame, IN 46556, USA
M. Aubouy
Spram CEA, 17 av. des Martyrs, 38054 Grenoble Cedex, France
F. Graner
CNRS UMR 5588 et Université Grenoble I, Laboratoire de Spectrométrie Physique, BP 87, F-38402 St Martin d'Hères Cedex, France

Abstract: In 2D random foams we define the mesoscopic stress and strain, which we measure directly from foam images. We evaluate the mesoscopic definition in static foams. Comparing the shear flow of monodispersed and polydispersed foams, we discuss the stress-strain relationship in the elastic regime and the transition between the elastic and flow regimes.

1 Introduction

Foams and emulsions are complex fluids with one phase (gas or fluid) dispersed in a continuous fluid phase [1]. Small perturbations to the Newtonian behavior of the continuous phase can describe the shear rheology of dilute dispersions. Highly concentrated dispersions, on the other hand, exhibit very complex rheology, from solid-like characteristics such as finite shear modulus and yield stress, to non-Newtonian viscosity [2, 3]. The rheological properties of concentrated dispersions, such as fluid foams or concentrated emulsions differ drastically from those of their constituent components. Packing and jamming of bubble structures become crucial when the flow requires bubble rearrangement [4]. How can we predict the mechanical properties of a foam (we use the term loosely to include all concentrated dispersions) from its structure?

A comprehensive theoretical understanding of the rheological properties of real foams must account for bubbles' varying sizes, disordered structure and rearrangement dynamics. Constitutive theory thus far works only for idealized periodic arrays of bubbles. For periodic monodispersed hexagonal foams and polydispersed hexagonal (small area disorder) foams, Khan and Armstrong, Reinelt and Kraynik *et al.* have derived a constitutive stress at the microscopic level, which can be averaged over unit cells to yield the macroscopic stress tensor [2, 3, 5]. The difficulty of a constitutive approach for real foams lies in quantifying the random foam structure. Recently we have derived a systematic approach to estimating the equilibrium energy and configuration of 2D random foams [6]. We define, for the first time, a stress and strain at the mesoscopic level for random foams, which average to yield macroscopic stress. We test these definitions in both foam flow experiments and shear foam simulations.

2 Methods

We study both 2D experimental soap foams and simulated Potts model foams.

We create the soap foam by blowing air bubbles into surfactant solution (usually 2% by volume Dawn brand liquid dishwashing detergent and 1% glycerin in de-ionized water). Trapped between two horizontal, parallel glass plates, measuring $10cm \times 10cm$ with a $0.7mm$ separation between plates, the foam is quasi two-dimensional. Figure 1a shows a schematic of the flowing foam apparatus: the aqueous foam flows through a quasi-two-dimensional chamber. The rate of introduction of bubbles into the apparatus controls the flow rate. Forcing the foam through a narrow constriction at the end of the flow chamber creates shear in the otherwise steady flow. A digital camera and a frame capture board capture and store foam images. Custom developed software allows us to identify and track each bubble during the flow. Figure 1b shows the trajectories of bubbles from 100 images. Furthermore, we can also collect information about each vertex and determine both the occurrence and the location of topological events.

We also allow these two-dimensional foams to coarsen towards the disordered scaling state [7]. Figure 1c shows one typical intermediately disordered fully equilibrated foam pattern.

Detailed descriptions of 2D foam simulations using the extended large-Q Potts model have appeared elsewhere [6, 9]. In this study, we apply bulk shear by a different method. With periodic boundary conditions in $\hat{x}$ and non-slip boundary conditions in $\hat{y}$, we copy the lattice spins in the direction of increasing x at a rate proportional to their y coordinate value. The strain rate is the speed of spin copying divided by the perpendicular distance to the zero speed line. Figure 2 shows a typical random foam under bulk shear; the strain rate corresponds to $\tan\alpha$.

3 Formalism

We consider 2D dry foams with fixed bubble areas, assuming that the shear is much faster than foam coarsening. We also assume that the size and topological disorder is small enough that our microscopic reference length L is well defined (see below) but large enough that the polydispersed foam is macroscopically homogeneous and isotropic. Our formalism generalizes to foams with arbitrary polydispersity, fluid fraction, and varying bubble size such as for compressible bubbles, bubble annihilation, nucleation, division and coalescence. We assume that foams are quasistatic (*i.e.* shear is much slower than the relaxation of films) so Plateau's rules hold at all times (*i.e.* bubble edges are arcs of circles which meet in triples at $2\pi/3$ angles).

We introduce a mesoscopic scale D, corresponding to the size of a "fluid particle" in hydrodynamics, over which averages dominate fluctuations so we can treat the foam as continuous. In statics, D must be much larger than both the correlation length of the bubbles (*i.e.* the largest bubble size) and of the film orientations. In flowing foams with bubble rearrangements, D must be larger than the size of the largest rearranging bubble cluster. Figure 1c shows on top of a disordered foam, grid lines indicating the mesoscopic lengthscale D. Each grid box is a unit cell in which the foam is approximately continuous. Large bubbles require coarse grids while finer grids suffice for smaller bubbles. Ultimately, the mesoscopic lengthscale should scale out and not affect the measured local stress and

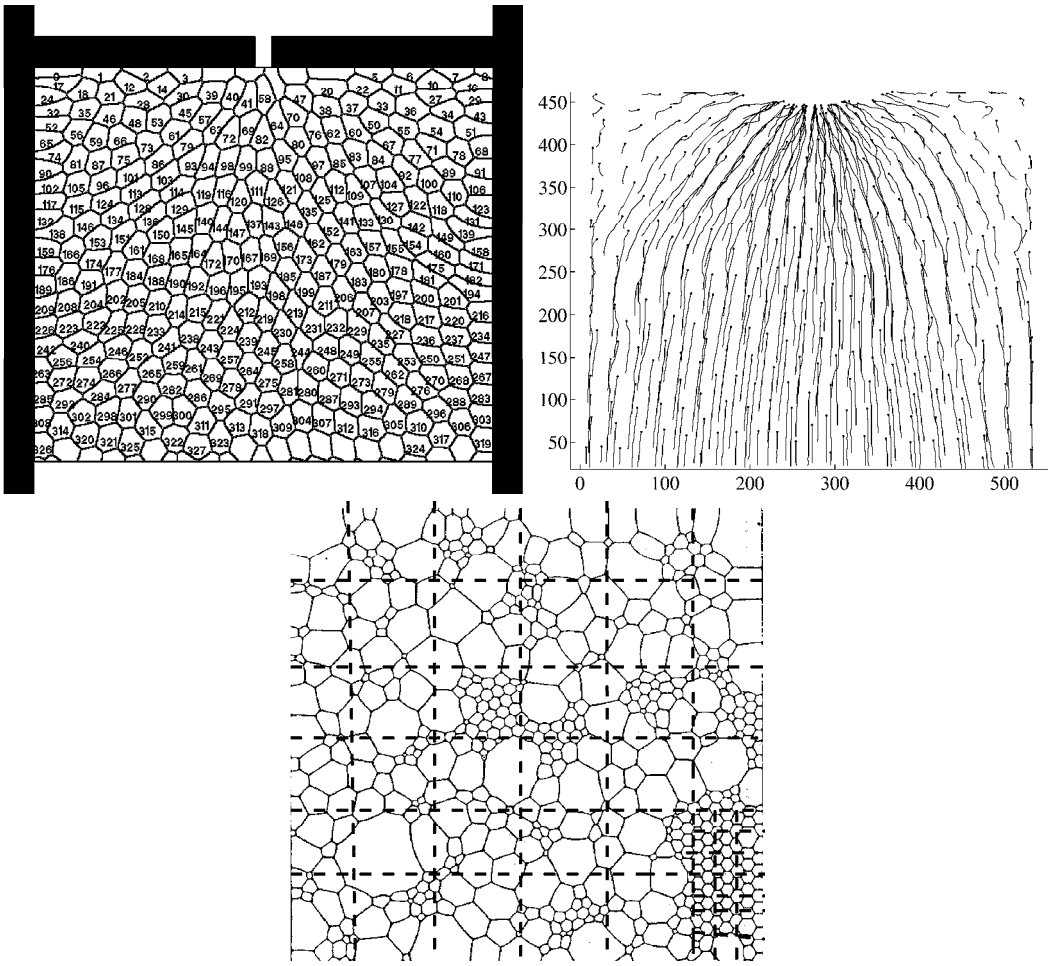

Figure 1: Experimental two-dimensional foams. a. Simplified schematic of flow apparatus with an analyzed image, numbers indicating different bubbles. b. Trajectories of bubbles from 100 images. c. A foam at an intermediate stage of coarsening, disordered and equilibrated. Dashed grid lines indicate the mesoscopic length scale, D (see Section 3).

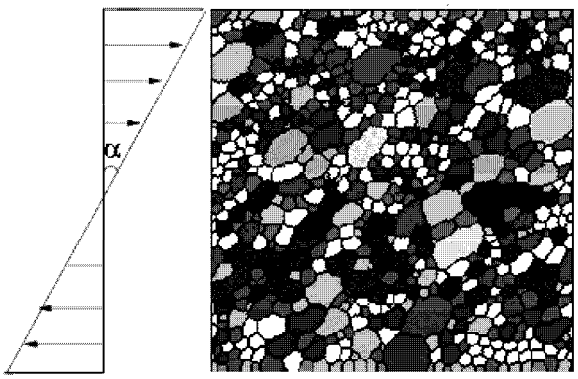

Figure 2: Simulated two-dimensional foam under bulk shear. The schematic on the left shows the strain rate profile across the foam. The strain rate of the foam is the slope of the profile, $\tan\alpha$.

strain.

In an equilibrated foam, detailed force balance dictates that all bubble films have the same stress force f. Thus the force on a box is the sum of all stress forces exerted by the films pulling on the 'box,' which vary with position, time, and orientation of the film elements. Thus the stress on the box due to surface tension is:

$$\sigma^s = \frac{f}{D} \sum_{ij} \hat{e}_i \otimes \hat{e}_j, \tag{1}$$

where $\hat{e}$ is the unit vector tangent to the films crossing the grid box, which we can determine from the foam image. Thus the stress due to surface tension is a symmetric tensor, whose trace is proportional to the density of films, *i.e.* to the number density of bubbles within the box.

The instantaneous macroscopic stress for the foam is the average of the local stress over the grid boxes. It has both non-dissipative and dissipative parts. The non-dissipative (*i.e.* static) stress is [2, 3]:

$$\sigma^{nd} = \sigma^p + \sigma^s, \tag{2}$$

where,

$$\sigma^p = \frac{1}{A} \sum_i (-P_i), \tag{3}$$

is the average bubble pressure within the box, and A is the area of the box. This pressure term comes from the bubble pressure and the capillary pressure in the Plateau borders [2]. The former determines the curvature of each film according to Laplace's law. The latter is proportional to fluid viscosity [8]. The dissipative part relates to foam's fluid properties and applies only to flowing foams.

Formally, we define the strain u as the conjugate variable to stress σ with respect to the free energy F:

$$dF = \sigma du. \tag{4}$$

Thus strain is undefined up to an additive constant. For a random foam, we conjecture that we can define a local strain by averaging over many films. Empirically, we define the local strain at the mesoscopic length scale D as:

$$u = \sum_{ab} (\frac{l_{ab}}{L_{ab}} - 1) \hat{e}_i \otimes \hat{e}_j, \tag{5}$$

where l_{ab} and L_{ab} are the real and reference lengths of the film between bubbles a and b, respectively; $\hat{e}$ is again the unit vector tangent to the films crossing the grid box. The reference length L_{ab} is a function of the areas of bubbles a and b [6]. $l > L$ corresponds to a stretched film and $l < L$ corresponds to a compressed film. Thus this definition of strain depend only on the present vertex positions and does not require knowing vertex positions at equilibrium. At equilibrium l_{ab} on average tends to L_{ab} [6] and the strain tends to zero.

Averaging local stress and strain yields the macroscopic stress and strain. The macroscopic shear stress is $\langle \sigma_{xy} \rangle$, averaged over all grid boxes, and the macroscopic normal stress, or hydrostatic pressure is $\langle Tr(\sigma) \rangle = \langle \sigma_{xx} + \sigma_{xy} \rangle$, the trace of the stress tensors averaged over the whole foam.

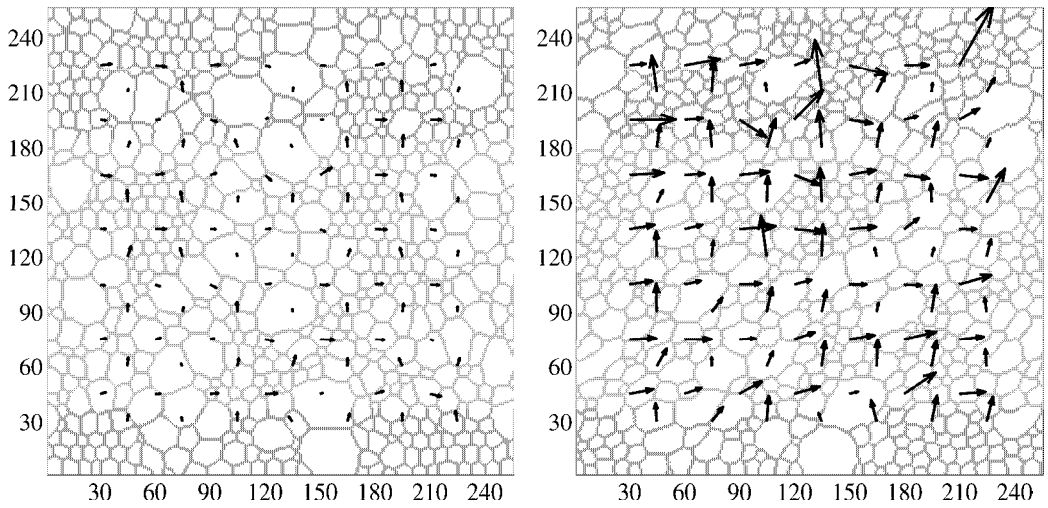

Figure 3: Distribution of local stress shown as vectors. a. Stress in a static foam. b. Stress in a sheared foam. Vector lengths enlarged 100 times to show details.

4 Static Foams

We measured the stress and strain on fully equilibrated foam images resembling Figure 1c. Both global and local stresses are zero with fluctuations (data not shown), as we expect.

Figure 3a shows a simulated equilibrated foam (lattice size 256×256). A mesh of size $D = 30$ (larger than the size of the largest bubble) overlays the image. The arrows show the distribution of local stress components: the vertical arrows show $\vec{\sigma}_i = \sigma_{ii}\hat{e}_i + \sigma_{ij}\hat{e}_j$, and the horizontal arrows, $\vec{\sigma}_j = \sigma_{ji}\hat{e}_i + \sigma_{jj}\hat{e}_j$. We have enlarged the arrows by a factor of 100 to show detail. Figure 3b shows the same foam after shear. The vectors on the overlay mesh of size $D = 30$ show the local stress components $\vec{\sigma}_i$ and $\vec{\sigma}_j$. The arrows, corresponding in length to the magnitude of local stress, are significantly longer than in the equilibrated case. The averaged macroscopic hydrostatic pressure, $\langle Tr(\sigma)/2\rangle = 0.001\gamma$ for the equilibrated foam, and $\langle Tr(\sigma)/2\rangle = 0.08\gamma$ for the sheared foam, where γ is the surface tension. The latter is much larger than the former, as we expect.

To illustrate the distribution of stress tensors, we calculated the eigenvalues λ_1, λ_2 and eigenvectors $\vec{a}_1, \vec{a}_2$ of the local stress tensors σ_{ij}. Figure 4 shows the stress tensors from the steady foam flow experiments, averaged over 2000 frames. We present the local stress tensors as ellipses, with the major and minor axes corresponding to $\lambda_1\vec{a}_1$ and $\lambda_2\vec{a}_2$, respectively.

5 Dynamic Foams

The response of foam under shear falls in two distinct regimes: the elastic regime where the bubbles deform elastically but no bubble rearrangements occur, and the flow regime where bubble rearrangements result in constant dynamic changes in film lengths.

In the elastic regime, the stress (eq. 1) is linearly proportional to the strain (eq. 5) [10], with the proportionality the Young's modulus. In the flow regime, however, u no

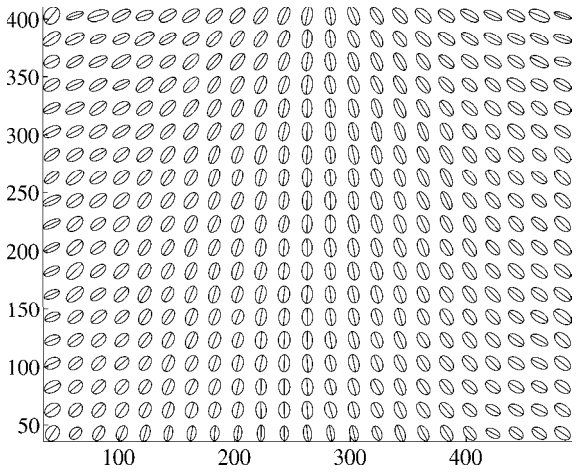

Figure 4: Stress distribution in foam flow through a constriction, corresponding to Figure 1a. The major and minor axes of the ellipses are eigenvectors of the local stress tensors, their magnitudes proportional to their eigenvalues.

longer defines the strain. Because T1 events destroy old films and create new ones, film lengths vary discontinuously so the reference length L ceases to be meaningful. The time derivative, $\dot{u}$, then should include both the elastic variations of film length l and the dynamic variation of L. We introduce a *topological* tensor T to account for this effect of T1 events:

$$V_{ij} = \dot{u}_{ij} + T_{ij}, \tag{6}$$

where V is the gradient of the velocity field $\vec{v}$,

$$V_{ij} \equiv \frac{d\vec{v}_i}{d\hat{e}_j}. \tag{7}$$

T relates to the rate of T1s per unit area. We conjecture that T depends only on $\hat{e}_i \otimes \hat{e}_j$ and that $Trace(T) = 0$. For steady flow, u is time independent [11], hence:

$$V = T, \tag{8}$$

i.e. the gradient of the velocity field is equivalent to the T1 rate. Figure 5 shows that in foam flow experiments, both the velocity gradients and T1 rates increase near the constriction.

Figure 6 shows the stress-strain curve from simulated foams for the transition between elastic and flow regimes. We apply bulk shear to a monodispersed hexagonal foam: as the strain increases, the average shear stress increases nearly linearly until at a strain of approximately 0.3, the *yield strain*, T1 events begin and the foam flows. The accumulated shear stress drops in response and then fluctuates around a steady value independent of the increasing strain. The foam flows like a fluid. On the other hand, the average hydrostatic pressures are independent of shear strain.

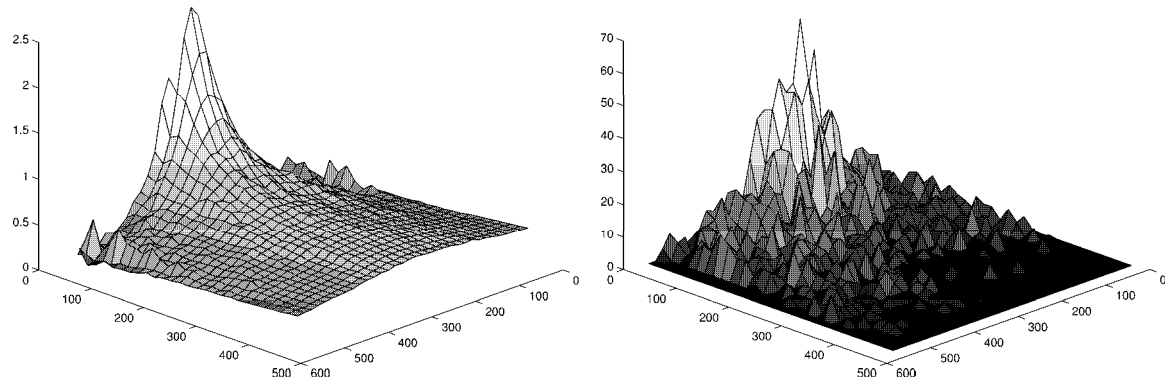

Figure 5: Steady foam flow experiment. Left: Speed distribution. Right: T1 rate, the number of T1 events per unit time per unit area.

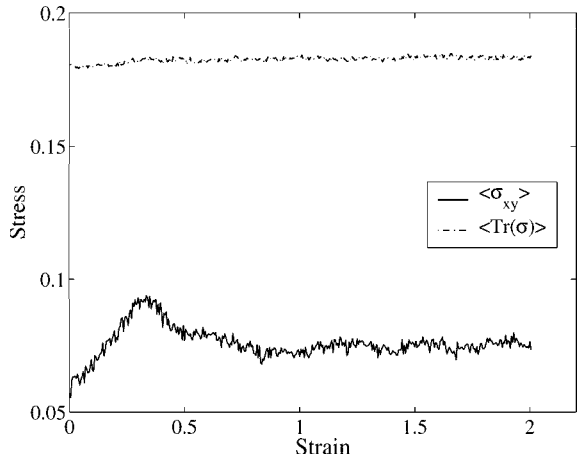

Figure 6: Stress-strain plot of simulated foams for a monodispersed foam. Dotted line is average pressure and solid line is average shear stress.

6 Summary

We have defined stress and stain at a mesoscopic scale, for 2D equilibrium random foams and out-of-equilibrium, flowing foams. These definitions allow direct measurement of local stress and strain from foam images.

We have presented the first full stress and strain distributions for a flowing foam. More detailed analysis will determine whether force chains form in foams as they do in granular materials [12]. Averaging the local stress and strain over the mesoscopic length scale yields the macroscopic stress and strain, which we can then compare to experimental stress-strain measurements.

Acknowledgments: Jiang is supported by DOE under contract W-7405-ENG-36. Glazier and Asipauskas acknowledge support from DOE grant DE-FG0299ER-45785, NASA grant UGA99-0083, NSF grants DMR92-57011, CTS96-01691 and INT96-03035-OC.

References

[1] A. M. Kraynik, Ann. Rev. Fluid Mech. **20**, 325 (1988).

[2] D. A. Reinelt, A. M. Kraynik, J. Fluid Mech. **215**, 431 (1990).

[3] A. M. Kraynik, D. A. Reinelt, H. M. Princen, J. Rheol **35**, 1235 (1991).

[4] A. Staint-Jalmes, D. J. Durian, J. Rheol. **43**, 1411 (1999).

[5] S. A. Khan, R. C. Armstrong, J. Non-Newtonian Fluid Mech. **22**, 1 (1986).

[6] F. Graner, Y. Jiang, E. Janiaud, C. Flament, Phys. Rev. E, in press (2000).

[7] J. A. Glazier, *The Evolution of Cellular Patterns*, Ph.D. dissertation, U. Chicago (1989).

[8] K. J. Mysels, K Shinoda, S. Frankel, *Soap films: Studies of their thinning*, Pergamon (1959).

[9] Y. Jiang, P. J. Swart, A. Saxena, M. Asipauskas, J. A. Glazier, Phys. Rev. E **59**, 5819 (1999).

[10] S. Alexander, Phys. Reports **296**, 65 (1998).

[11] G. Porte, J.-F. Berret, J. Harden, J. Phys. II France **7**, 459 (1997).

[12] Y. Jiang, F. Graner, in preparation.